



Effects of COVID-19 lockdown on water quality, microbial extracellular enzyme activity, and sediment-P release in the Ganga River, India

Madhulika Singh¹ · Usha Pandey² · Jitendra Pandey¹

Received: 30 November 2021 / Accepted: 9 April 2022 / Published online: 18 April 2022
© The Author(s), under exclusive licence to Springer-Verlag GmbH Germany, part of Springer Nature 2022

Abstract

This study investigates possible improvement in water quality and ecosystem functions in the Ganga River as influenced by COVID-19 lockdown in India. A total of 132 samples were collected during summer-2020 low flow (coinciding COVID-19 lockdown) for water (sub-surface and sediment-water interface) and 132 samples separately for sediment (river bottom and land-water interface) considering 518-km main river stem including three-point sources (one releases urban sewage and the other two add metal-rich industrial effluents) and a pollution-impacted tributary. Parameters such as dissolved oxygen deficit and the concentrations of carbon, nutrients (N and P), and heavy metals were measured in water. Sediment P-release was measured in bottom sediment whereas extracellular enzymes (EE; alkaline phosphatase, FDAase, protease, and β -D-glucosidase) and CO₂ emission were measured at land-water interface to evaluate changes in water quality and ecosystem functions. The data comparisons were made with preceding year (2019) measurements. Sediment-P release and the concentrations of carbon, nutrients, and heavy metals declined significantly ($p < 0.05$) in 2020 compared to those recorded in 2019. Unlike the preceding year, we did not observe benthic hypoxia (DO < 2.0 mg L⁻¹) in 2020 even at the most polluted site. The EE activities, which declined sharply in the year 2019, showed improvement during the 2020. The stability coefficient and correlative evidences also showed a large improvement in the water quality and functional variables. Positive changes in functional attributes indicated a transient recovery when human perturbations withdrawn. The study suggests that timing the ecosystem recovery windows, as observed here, may help taking management decision to design mitigation actions for rivers to recover from anthropogenic perturbations.

Keywords COVID-19 · Extracellular enzymes · Ganga River · Metal pollution · Hypoxia · Recovery window

Introduction

The coronavirus pandemic, commonly known as COVID-19 pandemic, emerged as a serious threat to human health in 2020 and continued in 2021. This infection disease was first identified on 31st December, 2019, in Wuhan, China, with the symptoms of unexplained multiple respiratory disorders.

The World Health Organization declared the COVID-19 as a pandemic on 11th March, 2020, as the transmission rate increased by 13 folds and 114 countries showed thousands of positive cases and number of deaths (WHO 2020). To slowdown the rate of infection, global countries adopted the lockdown to restrict human mobility. The Government of India imposed the lockdown in three phases in continuation from March 23rd to May 17, 2020, that completely restricted the social, economic, and urban-industrial activities. This period could be expected to show improvement in water quality and ecosystem responses in surface water bodies (Gard et al. 2020; Karunanidhi et al. 2021; Chakraborty et al. 2021a; Khan et al. 2021). Because of the longitudinal heterogeneity in rivers, evaluation of temporal and spatial patterns of water quality and microbial functional attributes is important. It helps in identifying changes in environmental determinants that alter biogeochemical control along the river continuum under the prevailing global change scenario

Responsible Editor: Xianliang Yi

✉ Jitendra Pandey
jiten_pandey@rediffmail.com

¹ Ganga River Ecology Research Laboratory, Environmental Science Division, Centre of Advanced Study in Botany, Institute of Science, Banaras Hindu University, Varanasi 221005, India

² Department of Botany, Faculty of Science and Technology, Mahatma Gandhi Kashividyapith University, Varanasi 221002, India

and local perturbations (Zeglin 2015; Jaiswal et al. 2021). Under undisturbed natural conditions, the downstream biogeochemical attributes are strongly regulated by upstream fluxes and processes. Under anthropogenic controls, lateral flushing of pollutants dramatically alters the water quality and ecosystem functions downstream. In addition to water quality changes, sediment characteristics are also altered considerably. Strong mechanistic linkages and correspondence between water quality and sediment quality variables suggest the need to understand how the water quality and sediment microbial attributes — such as EE activities and feedbacks — respond to changes in anthropogenic-environmental controls during the pandemic. These attributes blend conditions in course of time (Hill et al. 2010; Jaiswal and Pandey 2019a).

River ecosystems are strongly influenced by downstream hydrologic flow with a consistent pattern of loading and utilization of nutrients and organic matter along the gradient (Vannote et al. 1980). After the emergence of the theory of river continuum (Vannote et al. 1980), many researchers reported nutrient and organic matter metabolism along the continuum (Bournaud et al. 1996; Maranger et al. 2005; Zoppini et al. 2014). Most of the studies supporting the river continuum concept highlight the role of watershed factors rather than site-specific conditions resulting from local environmental controls (Wallace et al. 1997). Studies, particularly those focusing on the consequences of the anthropogenic perturbations, advocate that strong modifications result in river-water and sediment characteristics due to lateral entry of human releases (Jaiswal and Pandey 2021b; Jaiswal et al. 2021). Contexting to organic matter degradation, some studies have highlighted interactive roles of microbial extracellular enzyme (EE) activities and local determinants along the continuum (Sinsabaugh et al. 2002, 2009; Jaiswal and Pandey 2019a). The other researchers and conceptual models show spatial variability, including those in regulatory determinants (source of carbon and nutrients etc.) and functional attributes (extracellular enzymes, microbial response diversity etc.) along the river continuum (Maranger et al. 2005; Kobayashi et al. 2009; Savio et al. 2015; Zeglin 2015; Freixa et al. 2016). The spatial variability is particularly relevant for rivers which are subjected to water regulation and lateral entry of human releases. The anthropogenic flushing alters water and sediment quality and, depending upon the nature of input, affects microbial metabolism along the river continuum (Hill et al. 2010; Zeglin 2015; Jaiswal et al. 2021).

The microbial biomass constitutes the trophic base in detrital foodwebs (Manzoni et al. 2008; Sinsabaugh et al. 2009) and the EEs reflect the efficiency of microbial assimilation of carbon and nutrients (Sinsabaugh et al. 2009, 2016; Hill et al. 2010) and the presence of inhibitors (Jaiswal and Pandey 2019a). The EEs are used

as functional measures of microbial community metabolism. Because EE expression reflects cellular metabolism regulated by environmental variability and proportion of carbon and nutrients, they are used as proximate agents of biogeochemical processes and the prevailing environmental conditions (Schimel and Weintraub 2003; Sinsabaugh et al. 2016; Hill et al. 2010). Furthermore, because the distribution of EEs demarcates the boundaries of microbial responses to disturbances (Jaiswal and Pandey 2019a) and fluctuations in environmental resource availability (Hill et al. 2010; Sinsabaugh et al. 2009; Luo et al. 2017), the EE activities can be used to identify resource distribution or inhibitors constraints in metabolic scaling of microbial responses in context of the anthropogenic releases. Three groups of enzymes — glycosidases, peptidases, and esterases — are commonly used as a proxy of carbon and nutrient acquisition in the river sediments (Hill et al. 2010). The glycosidases mediate cleavage of glycoside bonds to release carbon, peptidases cause protein degradation and N release, whereas esterases cause enzymatic cleavage of ester bonds associated with phosphorous and sulfur acquisition.

The understanding of how an ecosystem “responds” to dynamic interactions of multiple factors is fundamental to predict future effects of anthropogenic-environmental changes (Jaiswal et al. 2021). Accordingly, this study attempted to ascertain the longitudinal patterns in water quality, sediment microbial responses, and sediment-P release as influenced by reductions in lateral input of human releases during lockdown period of COVID-19 (2020). These changes/responses were compared with the results obtained during pre-lockdown period (2019) to quantitatively evaluate the differences in context of lockdown period-associated reductions in the concentrations of carbon, nutrients, and heavy metal pollutants. Collation of spatio-temporal dynamics in the concentration of pollutants linking mechanistically the water and sediment quality changes and response determinants under episodic decrease in nutrients, organic matter, and heavy metal supply (lockdown period) likely help timing the ecosystem recovery windows, although so far unproven. This novel aspect is addressed in this study. It is hypothesized that the changes in river and sediment quality together with ecosystem feedback — sediment-P release, and microbial response attributes — EE activities, along the river gradient subject to episodic reductions in the lateral inputs during COVID-19 lockdown, could help timing ecosystem recovery windows. Greater differences between sewage flushing sites and metal polluting industrial input locations could be expected owing to large reduction in the latter due to industrial shutdown, whereas the volume of carbon and nutrient-rich metropolitan effluent/sewage flushing, which favor EE activities, was not expected to decline in that proportion.

Materials and methods

The study area

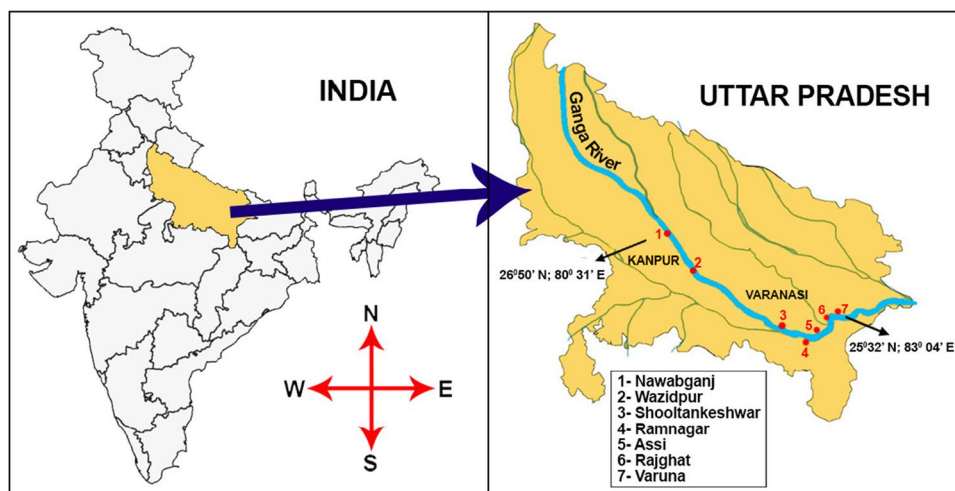
The study considers a 518-km-long transect of the Ganga River to investigate the influence of restrictions imposed during COVID-19 lockdown. Ganga, the largest river in India, traverses 2525 km from western Himalaya to the Bay of Bengal. The Ganga River Basin is the largest river basin in India (occupies ~26.2% of total geographical area). The lockdown-2020 in India coincides with summer season, a period wherein the river shows minimum discharge (relatively stable water surface) and maximum accumulation of pollutant elements. Accordingly, the study considers two consecutive summer seasons (2019 and 2020) for data comparison and to test whether the Ganga River experienced improvement in water quality/ecosystem functioning during lockdown-2020.

Experimental design and protocols

For detailed investigation, based on our previous studies, the land-water interface was considered as an imprint of changes/processes occurring in the river course (Jaiswal and Pandey 2019c). A total of 132 sediment samples and 132 water samples were collected from seven sites selected along the main river stem. Among these, three represents point sources — two associated predominantly with the industrial effluents and third one with the urban release (Fig. 1). Seven sites include as follows: (1) Nawabganj (Nwbj) located upstream Kanpur urban; (2) Wazidpur (Wpdr) receiving Kanpur industrial point source influence; (3) Shooltankeshwar (Shtk), least polluted site

characterized by rural-agricultural-woodland influence; (4) Ramnagar (Rmng) with the industrial point source influence; and (5), (6), and (7) respectively representing a point source (Assi drain; Asdr), a tributary (Varuna; Vrun), and a downstream Varanasi city site (Rajghat; Rjht). For sample collection and measurements of physical, chemical, and functional variables, the study followed identical protocols. Triplicate samples were collected from sub-surface water (15–25-cm depth) from three sub-sites of each site in the third week of the June each year. Sediment samples were collected in two sub-sets — one from the land-water interface (LWI) and other from the sediment-water interface from upper layer of the sediment (0–5-cm depth). For the LWI, a 2-m belt transect (1 m both side from zero reach) was used. For all sites, the samples were collected from three individual sub-sites and mixed to form composite samples. The water and sediment samples, contained in plastic bottles and acid-rinsed polyethylene bags, respectively, were placed in dark, in an icebox at 4°C and brought to the laboratory for further analysis. Water samples were acidified (1ml nitric acid/100ml) to avoid microbial acts on heavy metals. The sediment samples were divided into three parts. The first set was air dried at room temperature (3–4 days), grinded into a mortar, and sieved (2-mm mesh) to eliminate debris. The second part, considered for incubation studies, was preserved intact at 4°C. In the third set, freshly collected samples were incubated in a desiccator to maintain the moisture level at 80% for microbial extracellular enzyme, biomass/activity measurements. Data comparisons were made in two ways: spatial variabilities considering the least human impacted location (Shtk) as a reference site, and temporal variabilities considering lockdown (2020) vs non-lockdown (2019) period status of the river.

Fig. 1 Map showing study sites of Ganges River Basin



Measurements

Sub-surface water quality analysis

The biological oxygen demand (BOD) in sub-surface waters (15–25-cm depth) was quantified as BOD₅ (5-day incubation period; Eaton et al. 1995) and dissolved oxygen (DO) was measured following Winkler's method (APHA 1998). The chemical oxygen demand (COD) and the concentration of dissolved organic carbon (DOC) were estimated following potassium dichromate method (APHA 1998) and KMnO₄ digestion (Michel 1984) respectively. The dissolved oxygen deficit (DOD) was estimated following Sánchez et al. (2007) method. The water samples were collected from sub-water surface (15–25-cm depth) and the dissolved oxygen deficit was estimated as the difference between dissolved oxygen concentration measured at corresponding locations and the oxygen saturation concentrations of pure water at similar temperature and pressure. For determining the concentration of Cr, Cu, Cd, Zn, Ni, and Pb in water, a tri-acid digestion method (Allen et al. 1986) was followed. Samples in tri-acid mixture (high purity HNO₃ (70%), HClO₄ (65%), and H₂SO₄ (70%)) were digested in a microwave digestion system and filtered (Whatman No. 42). The concentrations determined using an AAS (Atomic Absorption Spectrophotometer; Analyst 800, Perkin Elmer).

Sediment quality analysis

Chemical analysis The CO₂ released from the sediment at the LWI was collected in known volume of steel chambers. The upper part of the chamber contains a rigid rubber fitted valve for collecting gas samples with the help of plastic syringe. The samples so collected were analyzed using a greenhouse gas analyzer (Trace 1110; Thermo Fisher Scientific, India). The data accuracy was ensured with repetitive calibration using standard gas. Total organic carbon (TOC) in the sediment was measured following Michel (1984), and soluble organic carbon (WSOC) was determined following the dichromate oxidation titrimetric method of Ciavatta et al. (1991). For NO₃⁻ and NH₄⁺ in sediment, the phenol disulphonic acid extraction method (Chapman 1996) and the phenate method (Park et al. 2009), respectively, were used. The phosphate concentration was estimated by ammonium molybdate method (Murphy and Riley 1962). For the determination of heavy metal contents, the dried sediment samples were subjected to digestion in a tri-acid mixture (H₂SO₄, HNO₃, and HClO₄ in 1:5:1 ratio, v/v). For this, high purity 70% HNO₃, 65% HClO₄, and 70% H₂SO₄ in a ratio of 5:1:1 (Allen et al. 1986) were used. This tri-acid mixture was added in a known volume of water sample and the solution was digested in a microwave digestion system (Model — MDS-6G; SINEO). The digested solution was then filtered

using a filter paper (Whatman No. 42) and the final volume was maintained up to 25 mL by adding distilled water and the values quantified in an AAS (The Perkin Elmer, Model Analyst 800, USA). The quality control, precision, and accuracy were achieved for all the measurements using drift blank and standard solution (Sisco Research Laboratory, India).

Microbiological activity For microbial biomass, the chloroform fumigation extraction procedure was followed. The sediment samples were separated into two parts: the first one was kept as non-fumigated and the second part was fumigated with CHCl₃ for 24 h. The microbial biomass-carbon (Cmic), biomass-phosphorus (Pmic), and biomass-nitrogen (Nmic) were estimated as per Jenkinson and Powlson (1976); Brookes et al. (1982); and Shen et al. (1984), respectively. The substrate-induced respiration (SIR) was determined by amending the samples with 6 mg of glucose per gram of sediment (Anderson and Domsch 1978) and the values expressed in terms of μg CO₂-C g⁻¹ h⁻¹. The microbial-metabolic-quotient (qCO₂) was quantified following Wardle et al. (1993).

Extracellular enzymes The alkaline phosphatase (AP) activity in sediment was measured following Tabatabai and Bremner (1969). The reaction mixture was prepared using freshly collected samples of sediment. A 2-g sediment sample was properly mixed with 1 M tris-hydrochloride buffer (with pH 8.6) and p-nitrophenyl phosphate (PNP) and aliquot incubated for 1 h at 37°C. After this, 0.5 N NaOH and 0.5 N CaCl₂ solutions were added to stop the reaction. After centrifugation (at 3000 rpm) for 10 min, the absorbance of the aqueous phase was recorded at 400 nm. The AP activity was expressed in terms of p-nitrophenol formed (μm p-NP g⁻¹ h⁻¹).

The fluorescein diacetate hydrolysis also was assayed spectrophotometrically (Adam and Duncan 2001). Freshly collected samples were taken for the experiment. A 2-g sediment sample was mixed with 60 mM solution of potassium phosphate buffer (pH 7.6) and 1000 μg fluorescein diacetate mL⁻¹ stock solution. The aliquot was shaken at 30°C with the help of a rotary shaker for 20 min. After that, the chemical reaction of experiment was stopped by adding chloroform:methanol (2:1, v/v) solution. The solution was then centrifuged at 2000 rpm and aliquot separated with the help of Whatman No. 1 filter paper. The absorbance was recorded at 490 nm using double beam spectrophotometer (model Systronic 2203). The fluorescein diacetate hydrolytic bioassay (FDAase) was expressed in terms of fluorescein formed (μmol fluorescence g⁻¹ h⁻¹).

For the β-D-glucosidase bioassay, the sediment samples were incubated with PNG (p-nitrophenyl-β-D-glucoside) and the p-nitrophenol formed was assessed

spectrophotometrically (Eivazi and Tabatabai 1988). The reaction mixture was prepared using 1-g sediment sample mixed with toluene, modified universal buffer, and the substrate (PNG). The aliquot was incubated for 1 h at 37° C. After that, it was mixed with 0.5 M CaCl₂ and 0.1 M tris-hydroxymethyl aminomethane (THAM). The aliquot solution was centrifuged at 3000 rpm and the absorbance was taken at 400 nm. A standard graph of p-nitrophenol was used to calculate the activity in terms of $\mu\text{g p-NP g}^{-1} \text{ h}^{-1}$.

The nitrogen mineralization enzyme protease was assayed in terms of aromatic acid formed on proteolytic cleavage of the casein and the values expressed as L-tyrosine equivalent (Ladd and Buttler 1972). For this, the reaction mixture was prepared using sediment sample, 0.1 M tris-HCl buffer and 1% casein as a substrate. The reaction mixture was mixed thoroughly and the solution was incubated at 49° C for 2 h. The Na₂CO₃ solution and 0.06% CuSO₄ solution were added in the centrifuged supernatant. After appropriate mixing, it was incubated for 30 min at room temperature. After this, Folin reagent was added and the solution was again incubated for 30 min (37° C). After incubation, the aliquot was centrifuged and the supernatant was used to record the absorbance at 578 nm. The protease activity ($\mu\text{g L-tyrosine g}^{-1} \text{ h}^{-1}$) was measured from standard graph of tyrosine.

The nitrate reductase (NR), a nitrogen assimilating enzyme, was measured spectrophotometrically (Nowak et al. 2002). The reaction mixture for NR consisted of 1-g fresh sediment sample, 1 mL 0.05 % KNO₃ solution, 1 mL of 0.8 mmol L⁻¹ 2,4-dinitrophenol, 1 mL 1 % glucose solution, and 7 mL of anaerobic deionized water. The reaction mixture was incubated at 30 °C for 24 h. Following incubation, it was filtered and the absorbance recorded at 520 nm. The activity for NR was expressed as mg NO₂⁻ N formed kg⁻¹ day⁻¹ of the sediment.

Statistical analysis

The ANOVA-interaction effects between parameters were used to evaluate the individual effects and interaction effects of the determinants. Correlative evidences were used to support shifts in relationships. Because variances between two sets of conditions could not be assumed to be equal, paired *t*-test was used to compare the means of different parameters measured under two separate scenarios (2019 vs 2020). Furthermore, because rising variance is often used as an indicator of ecological variability/ transition (Carpenter and Brock 2006), the stability coefficient (1/CV; the coefficient of variance) was used to visualize shifts in environmental perturbations (Kardol et al. 2018). The ordination plots were constructed using Non-Metric-Multidimensional Scaling (NMDS) to visualize spatial patterns in environmental and functional/response variables. For clarity, the water/

sediment quality “change” attributes are treated here as environmental variables. Effects of regulatory determinants on in-stream response variables (EE activity and sediment-P release) were tested using the generalized linear mixed models (GLMM). The GLMM allows both the fixed effects and the random effects. It allows establishing non-linear links between means of the response and predictors; models over dispersion; and correlations by incorporating the fixed effects with random effects (Breslow and Clayton 1993). For data analysis, statistical software- R (Version 4.1.2); Sigma-plot (version 11.0); PAST (version 2.17c); and IBM SPSS statistics 20 were used.

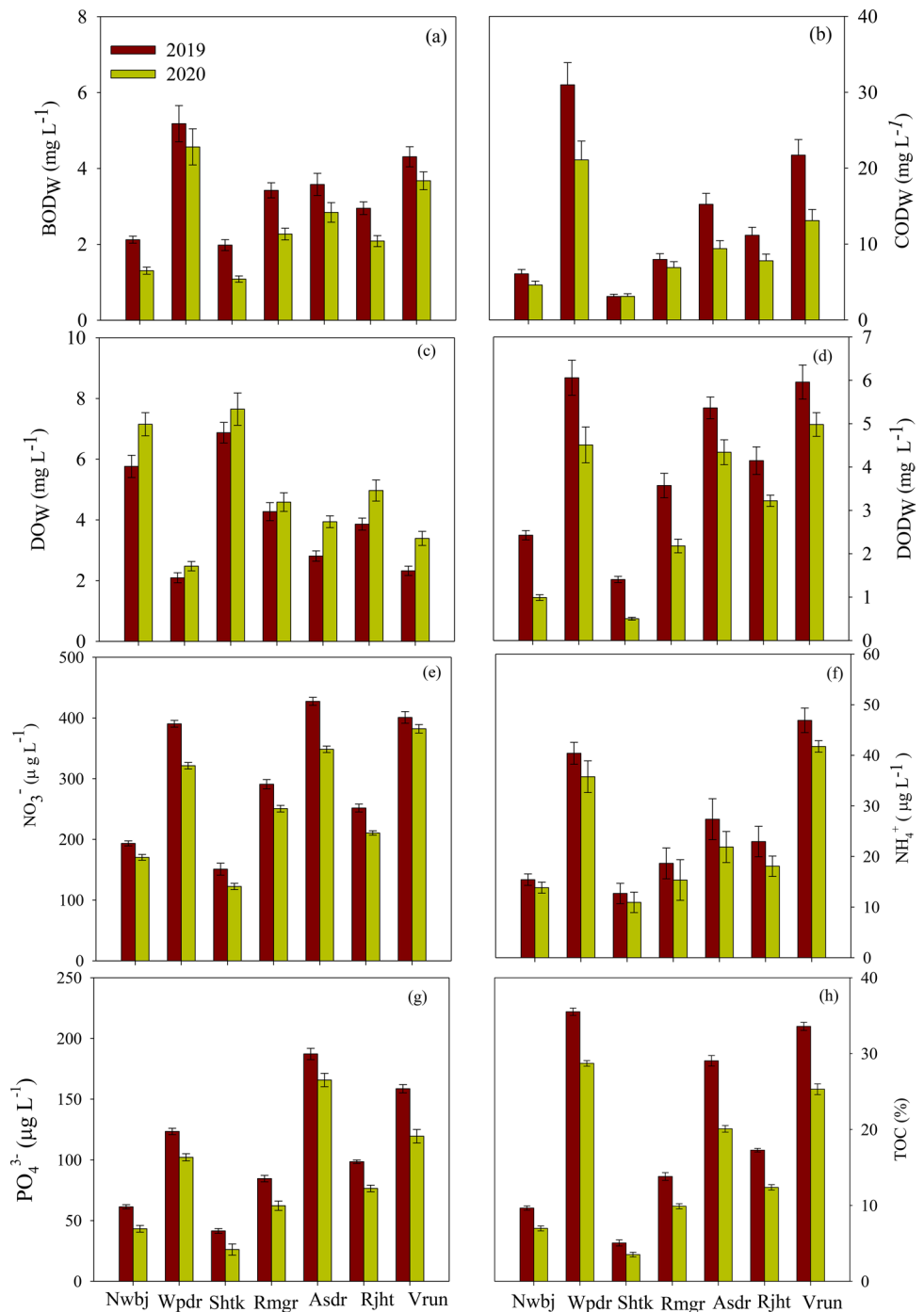
Results

Water quality determinants

According to the source input, the study sites may be broadly divided as follows: city site, industrial sites, tributary, relatively natural locations, and those with downstream urban-industrial influence. The Shooltankeshwar (Shtk) site with patches of agriculture mixed woodlands and minimum pollution pressure is considered here as relatively “natural” to present a reference condition for comparison with other “modified” locations. Spatial differences between sites were clearly evident with respect to the water quality attributes (Fig. 2). In the year 2019, the mean concentration of dissolved oxygen in water (DO_w) remained invariably lower at Wpdr (2.09 mg L⁻¹), Rmgr (4.27 mg L⁻¹), Asdr (3.86 mg L⁻¹), and Vrun (2.32 mg L⁻¹) compared to the values recorded at the reference site (6.87 mg L⁻¹). This trend continued but values increased significantly ($p < 0.05$) in the 2020. Biological oxygen demand (BOD) and chemical oxygen demand (COD) contrasted DO_w with values being highest (5.17 mg L⁻¹ and 30.97 mg L⁻¹, respectively) at Wpdr. The BOD and COD remained very low (1.08 mg L⁻¹ and 3.09 mg L⁻¹, respectively) at Shtk (Fig. 2). Dissolved oxygen deficit (DOD_w) showed strong synchrony with BOD ($R^2 = 0.84$; $p < 0.001$) and COD ($R^2 = 0.82$; $p < 0.001$). Concentrations of nutrients (NO₃⁻, NH₄⁺, and PO₄³⁻) and total organic carbon (TOC) were significantly ($p < 0.05$) higher at all locations during summer low flow of 2019 compared to those observed during the lockdown period (2020 summer low flow values). During 2019, the concentrations of inorganic-N (NO₃⁻ + NH₄⁺) were found to be 454.68 $\mu\text{g L}^{-1}$, 430 $\mu\text{g L}^{-1}$, and 447.67 $\mu\text{g L}^{-1}$ at Asdr, Wpdr, and Vrun, respectively. The PO₄⁺ at these respective sites remained above 125 $\mu\text{g L}^{-1}$ in 2019. In the year 2020, these values dropped significantly ($p < 0.05$).

The concentrations of study metals across sites showed concurrence with source attributes where the values were the highest at Wpdr and lowest at Shtk (Fig. 3). Heavy metal

Fig. 2 Sub-surface water quality — biological oxygen demand (BOD_w; **a**), chemical oxygen demand (COD_w; **b**), dissolved oxygen (DO_w; **c**), dissolve oxygen deficit (DOD_w; **d**), NO₃⁻ (**e**), NH₄⁺ (**f**), PO₄³⁻ (**g**), and TOC (**h**) at study sites. Values are mean (*n*=3) ±SE



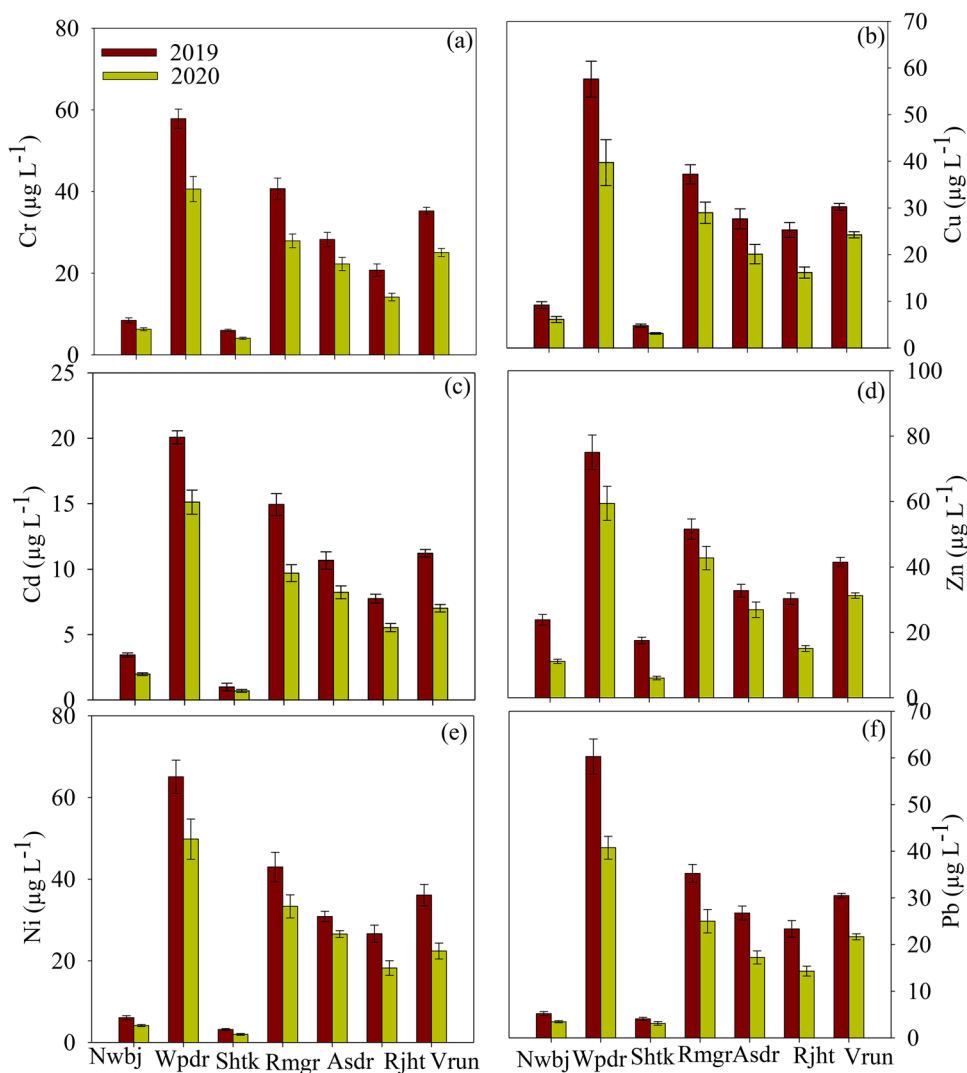
concentrations at study sites declined sharply in the year 2020. For individual metal, the concentrations from higher to lower ranges appeared as follows: Cr>Zn>Ni>Pb>Cu>Cd. Although the concentrations varied, this trend was found to be consistent at all the sites. When all the sites combined, for the individual metal, the values ranged as follows: Cr (4.05 to 57.81 µg L⁻¹), Zn (6.03 to 75.01 µg L⁻¹), Ni (1.96 to 65.04 µg L⁻¹), Pb (3.10 to 60.27 µg L⁻¹), Cu (3.11 to 57.61 µg L⁻¹), and Cd (0.69 to 20.07 µg L⁻¹). Concerning to total

heavy metal (ΣTHM), the overall values exceeded 337 µg L⁻¹ at Wpdr and remained below 37 µg L⁻¹ at Shtk.

Sediment variables at land-water interface

The chemical properties of sediments collected from the land-water interface (LWI) showed spatio-temporal variability almost imprinting the water quality attributes. Sediments at Asdr and Wpdr had considerably greater amounts

Fig. 3 Sub-surface water concentrations of heavy metals (a–f) at study sites of the Ganga River. Values are mean ($n=3$) \pm SE. Nwbj, Nawabganj; Wpdr, Wazidpur drain; Shtk, Sooltankeshwar; Rmgr, Ramnagar; Asdr, Assi drain; Rjht, Rajghat; Vrun, Varuna tributary

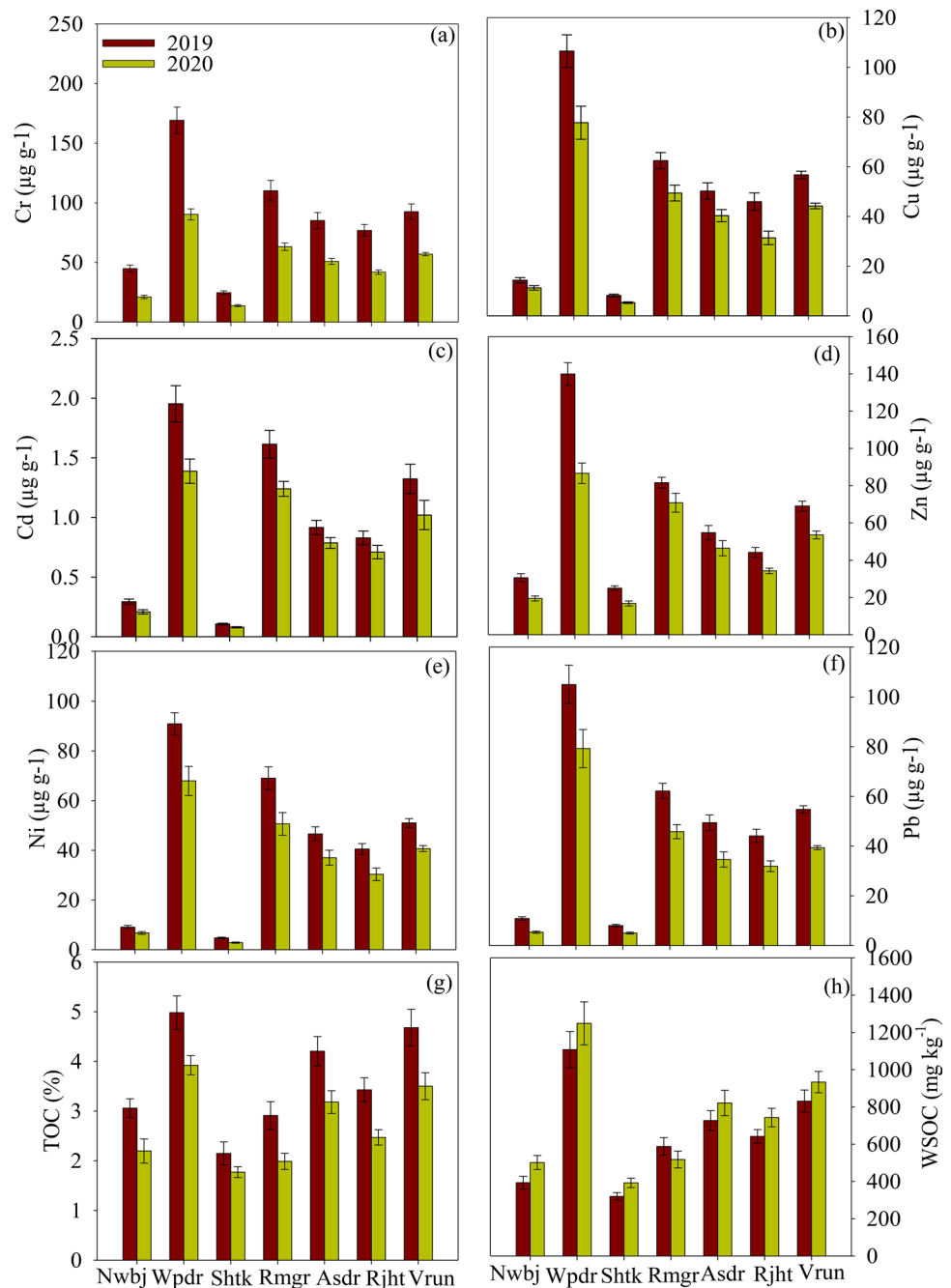


of TOC, NO_3^- , NH_4^+ , and PO_4^{3-} than those recorded at the other sites. Concentrations of sediment TOC and nutrients were significantly ($p < 0.05$) greater at all sites in the year 2019 compared to those of the 2020. These changes appeared more specifically marked at sites dominated by industrial point source compared to the other sites. At Wpdr (an industrial point source site), TOC, NO_3^- , NH_4^+ , and PO_4^{3-} in the sediment declined by 21.28, 34.34, 17.84, and 22.06% respectively in the 2020 compared to the 2019. The sediment-metal variations were large and showed strong dependence on source factors. Greater metal accumulation was observed in the year 2019 compared to the 2020, and more specifically at sites close to the point sources. Concentrations of heavy metals in the sediment showed synchrony with their respective concentrations in water (Figs. 3 and 4). Non-metric multidimensional scaling (NMDS) segregated ΣTTHM , TOC, and nutrients with highly polluted point sources and tributary (Fig. 5). Sediment-metal accumulation in the 2020 declined sharply, although this lockdown effect

did not able to switch the general trend of metal accumulation across-site. The ΣTTHM at Wpdr declined by 34.28% in the 2020 compared to the 2019. The stability coefficient computed for ΣTTHM , TOC, and microbial EE activity variables at the LWI was significantly ($p < 0.05$) higher in the 2020 compared to the 2019 (Table 1).

Microbial attributes, except metabolic quotient (qCO_2), contrasted with metal pollution load. The NMDS segregated microbial/EE activities opposite to ΣTTHM and qCO_2 irrespective of the year (Fig. 5). The microbial biomass (C_{mic}) and the substrate-induced respiration (SIR) remained lowest at Wpdr ($219.23 \mu\text{g g}^{-1}$ and $5.1 \mu\text{g CO}_2\text{-C g}^{-1} \text{h}^{-1}$ respectively) (Fig. 6). When compared with the C_{mic} measured in the 2019, significant ($p < 0.05$) increase was observed at all sites in the 2020. Opposite to C_{mic} and SIR, the CO_2 emission at the LWI remained higher in the 2019 compared to the 2020 (Fig. 6). The EE activities — β -D-glucosidase, protease, alkaline phosphatase, and nitrate reductase — all were lowest at Wpdr (Fig. 7).

Fig. 4 Concentrations of heavy metals (a–f), total organic carbon (TOC; g), and water soluble organic carbon (WSOC; h) in sediment at land-water interface at study sites of the Ganga River. Values are mean ($n=3$) \pm SE



Also, the activities were very low at Rmgr. Overall, the EE activities varied with site and except nitrate reductase, increased significantly ($p < 0.05$) in the 2020 compared to the 2019. The alkaline phosphatase showed asynchrony with PO_4^{3-} and the activity was maximum at Shtk (Figs. 6 and 7). The generalized linear mixed model (GLMM) analysis showed significant relationships between the variables, being negative with heavy metals. Also, AP activity correlated negatively with dissolved reactive P. With few exceptions, the relationships were stronger in the year 2019 (Tables 2 and 3). The multiparametric descriptive

analysis segregated EE activity opposite to the heavy metals (Fig. 8).

Sediment-water interaction

The COVID-19 lockdown also influenced the degree of interaction between water column and the river-bottom sediment. We consider DO at the sediment-water interface (DO_{sw}) and bottom sediment-P release to explore the implications of lockdown-driven changes in the river water chemistry on sediment-water interaction. Our results showed clear

Fig. 5 Non-metric multidimensional scaling (NMDS) segregating sites and study variables along the main stem of the Ganga River

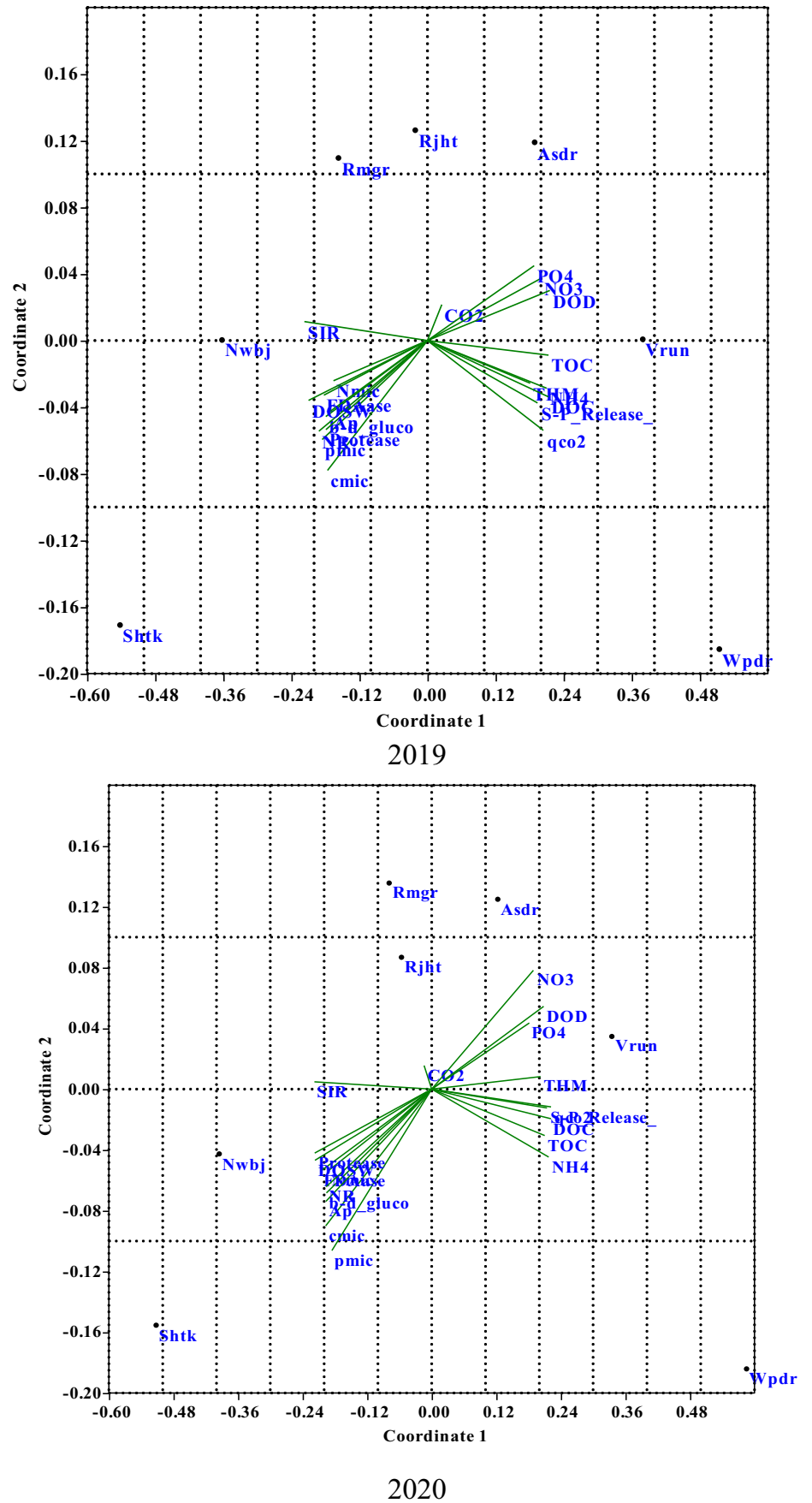


Table 1 The stability coefficients computed for different parameters measured for water and sediment at land-water interface of the Ganga River for the year 2019 and 2020

Variable																
Site	ΣHTM	WSOC	TOC	SIR	Cmic	Pmic	Nmic	PO ₄ ⁻	NO ₃ ⁻	NH ₄ ⁺	Glu	AP	FDAase	Protease	NR	qCO ₂ ⁻
2019																
Nwbj	0.14	0.16	0.16	0.15	0.18	0.16	0.18	0.11	0.16	0.19	0.17	0.19	0.16	0.18	0.16	0.20
Wpdr	0.03	0.04	0.04	0.03	0.05	0.03	0.04	0.03	0.04	0.05	0.03	0.04	0.02	0.03	0.04	0.03
Shtk	0.30	0.28	0.36	0.32	0.31	0.37	0.28	0.30	0.33	0.31	0.27	0.30	0.21	0.20	0.24	0.21
Rmgr	0.04	0.05	0.05	0.04	0.06	0.05	0.05	0.04	0.05	0.06	0.05	0.05	0.03	0.04	0.06	0.04
Asdr	0.07	0.06	0.08	0.07	0.08	0.07	0.07	0.06	0.07	0.08	0.07	0.07	0.06	0.07	0.08	0.08
Rjht	0.08	0.09	0.10	0.10	0.10	0.09	0.09	0.07	0.08	0.10	0.08	0.06	0.09	0.10	0.11	0.10
Vrun	0.05	0.07	0.06	0.07	0.07	0.06	0.06	0.05	0.06	0.07	0.06	0.06	0.05	0.06	0.07	0.06
2020																
Nwbj	0.22	0.26	0.27	0.37	0.29	0.24	0.25	0.27	0.30	0.29	0.27	0.24	0.29	0.28	0.29	0.32
Wpdr	0.07	0.09	0.08	0.07	0.08	0.07	0.07	0.07	0.07	0.08	0.06	0.07	0.06	0.06	0.07	0.06
Shtk	0.44	0.43	0.49	0.54	0.37	0.39	0.43	0.45	0.46	0.51	0.42	0.43	0.47	0.51	0.53	0.45
Rmgr	0.08	0.09	0.09	0.08	0.09	0.08	0.08	0.07	0.08	0.09	0.08	0.07	0.08	0.07	0.09	0.07
Asdr	0.10	0.11	0.11	0.10	0.11	0.10	0.10	0.09	0.10	0.11	0.10	0.09	0.10	0.10	0.11	0.11
Rjht	0.12	0.13	0.14	0.13	0.13	0.12	0.12	0.11	0.11	0.13	0.12	0.11	0.13	0.15	0.16	0.13
Vrun	0.09	0.10	0.10	0.10	0.10	0.09	0.09	0.08	0.09	0.10	0.09	0.08	0.09	0.09	0.10	0.09

The difference between respective stability coefficient (2019 vs 2020) is significant at $p < 0.05$ (t -test)

influence of source input on DO_{sw}, which remained the lowest (0.37 mg L⁻¹; 2019) at Wpdr and highest at Shtk (7.57 mg L⁻¹; 2020). The DO_{sw} increased in the 2020 irrespective of site (Table 4). The sediment-P release in the 2020 showed an opposite trend with the 2019 values being the highest (9.90 mg m⁻² day⁻¹) at Wpdr. The sediment-P release was found to be the lowest (0.66 mg m⁻² day⁻¹) in the 2020 at Shtk. The DO_{sw} showed significant improvement in the year 2020 lockdown and no benthic hypoxia (for instance, DO_{sw} below 2.0 mg L⁻¹) was observed even at the most polluted site. Accordingly, the sediment-P release in the 2020 declined sharply at all sites (Table 4).

Discussion

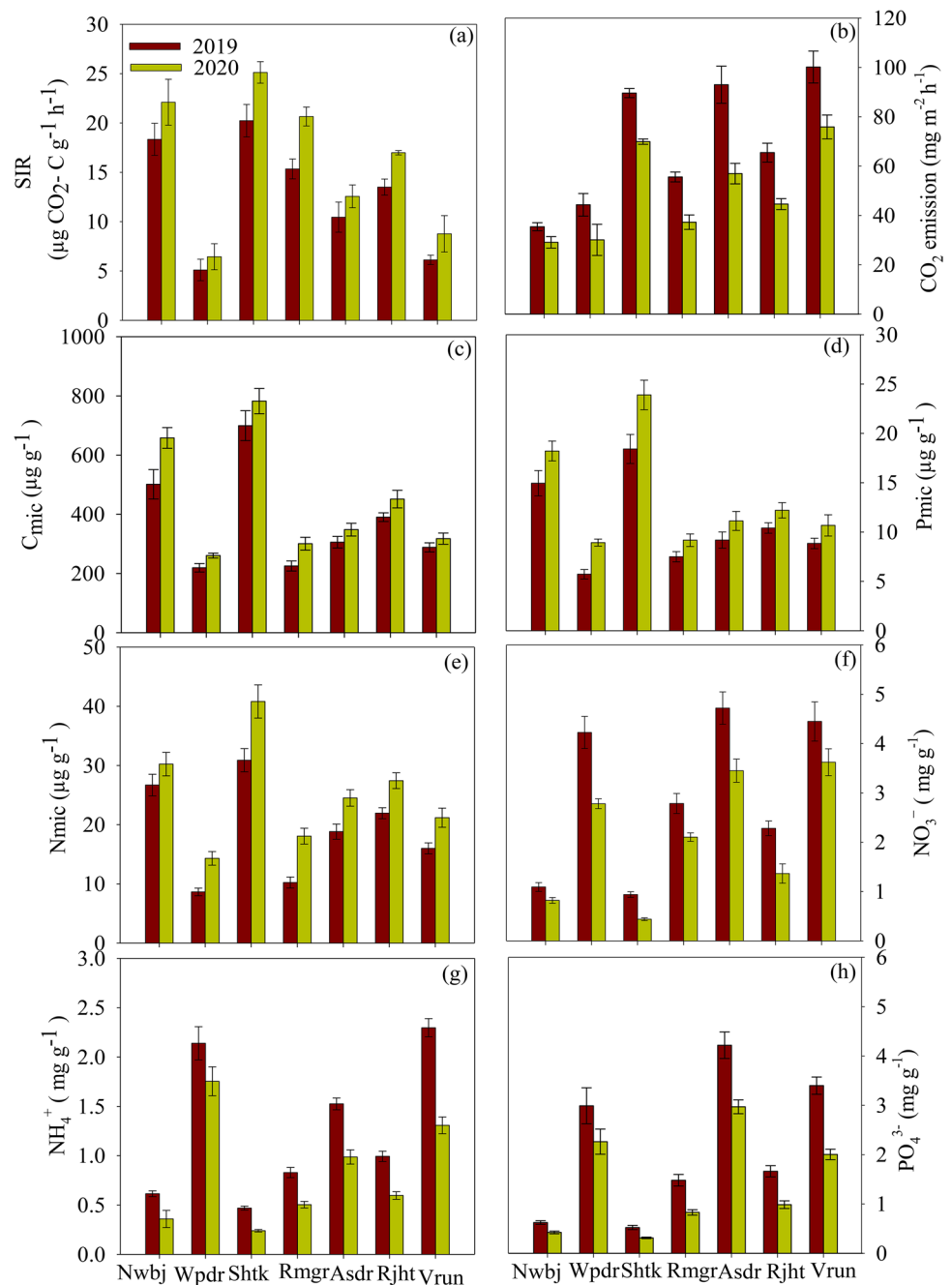
The rivers capture three dynamic and interconnected domains: atmosphere, land, and water, which control environmental conditioning and changes in water and sediment characteristics and heterogeneity of habitats which affect the microbial functional attributes in the system (Fazi et al. 2013; Freixa et al. 2016; Doherty et al. 2017). In anthropogenically impacted rivers, nutrients, heavy metals, and organic matter control the diversity of microbial functioning in the sediment along the river continuum (Freixa et al. 2016; Jaiswal and Pandey 2018). The period of COVID-19 enforcement of lockdown of industrial activities, tourism and road traffic etc., and associated reduction in the amount of wastes and pollutants, was expected to cause improvement

in the status of receiving water bodies. Available evidences support such expectations (Global Carbon Project 2020; Häder et al. 2020; Yunus et al. 2020). Here, based on two sub-sets of investigations — main river stem and point sources, the study shows that the Ganga River experienced significant improvement in water and sediment quality during COVID-19 lockdown period. Three-step comparisons were made to justify our results. These include as follows: spatial-source linked relationships; comparison of “change attributes” to “response determinants”; and comparison of the results with those generated during non-lockdown period (2019). Together with the common water quality variables, the study used dissolved oxygen at the sediment-water interface (DO_{sw}) and two response determinants — EE activities at the land-water interface, and release of P from the benthic sediment to decipher river ecosystem functioning and to mechanistically link the causal determinants.

Water quality changes

Accurate assessment of anthropogenic flushing and associated changes are often constrained due to lack of appropriate comparisons. The COVID-19 lockdown period can be used to compare the magnitude of common and specific anthropogenic influences on large rivers. The Ganga River water is withdrawn for agriculture sector usages along with drinking and domestic purposes. Our target here was to compare how and to what extent the period of COVID-19 enforcement of lockdown of industrial activities, tourism and road traffic

Fig. 6 Substrate-induced respiration (SIR; **a**), CO₂ emission (**b**), C_{mic} (**c**), P_{mic} (**d**), N_{mic} (**e**), NO₃⁻ (**f**), NH₄⁺ (**g**), and PO₄³⁻ (**h**) in sediment at land-water interface at study sites of the Ganga River. Values are mean ($n=3$) \pm SE



etc., and associated reductions in the amount of pollutants (carbon, nutrients, and heavy metals), were able to cause improvement in the water quality of the Ganga River. To validate our results, data comparisons were made with the preceding year (2019) measurements. Also, site-wise comparisons in water/sediment quality were made considering the least human-impacted site. An abrupt improvement in water quality observed here can be linked to non-functioning of such sources as restaurants, community halls, closure of schools and colleges, hostels, food stalls, tourism, traffic, business, and industrial activities together with reduced

disposal of wastes (Yunus et al. 2020; Karunanidhi et al. 2021). The concentration of dissolved oxygen in sub-surface water (DO_w) increased during lockdown period irrespective of study sites. The improvement in DO_w was noticed at upstream sites, downstream cities, and at point source locations. The effects at urban sites were relatively less marked. Here, the changes in discharge could be expected to be less pronounced during lockdown as also reported for other rivers in India (Khan et al. 2021). In a study of the Hoogly River Estuary, Chakraborty et al. (2021a) observed about 50% increase in the concentration of dissolved oxygen

Fig. 7 Activities of β -D glucosidase (a), FDAase (b), protease (c), alkaline phosphatase (d), nitrate reductase (e) activities, and microbial metabolic quotients (qCO_2 , f) at land-water interface at study sites of the Ganga River. Values are mean ($n=3$) \pm SE

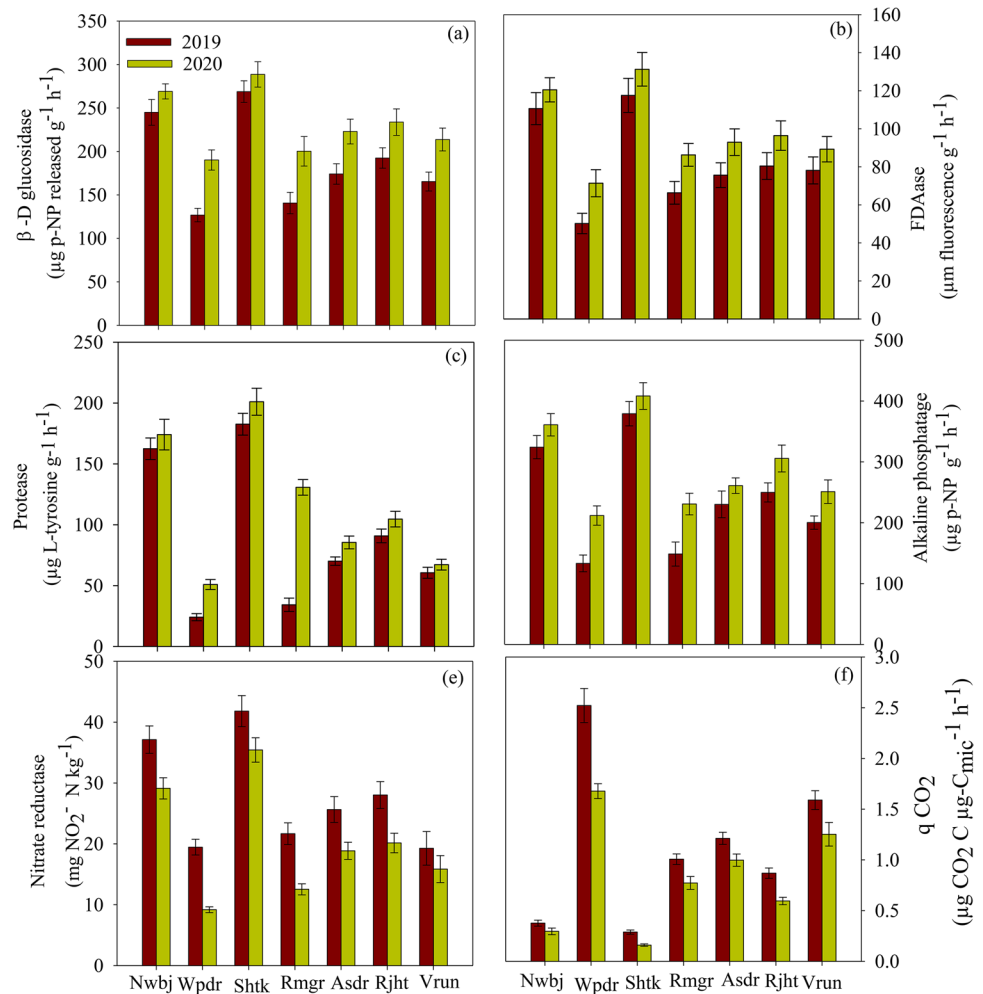


Table 2 Generalized linear mixed models (GLMM) to explain the patterns in extracellular enzyme activities in sediment at land-water interface (LWI) of the Ganga River in 2019

Variable	Slope of covariates				
	b_{TOC}	b_{IN}	B_{DRP}	$b_{\Sigma THM}$	Intercept
B-D-Glu	5.03***	4.84***	3.76***	-0.04***	18.97***
FDAase	5.92***	4.57***	3.12**	-0.03***	10.33**
Protease	4.84***	5.23***	3.46***	-0.04***	11.07**
AP	3.73**	3.71**	-3.80***	-0.04***	12.80***
NR	5.78***	7.69***	6.08***	-0.05***	30.81***

β -D-Glu, β -D-glucosidase; AP, alkaline phosphatase; NR, nitrate reductase; TOC, total organic carbon; IN, inorganic nitrogen ($NO_3^- + NH_4^+$); DRP, dissolved reactive phosphorus (PO_4^{3-}); ΣTHM , total heavy metal. The variance explained by both random (sites) and fixed effects (variables). Codes of significance: $p(>|t|)$: 0 “***”; 0.001 “**”.

Table 3 Generalized linear mixed models (GLMM) to explain the patterns in extracellular enzyme activities in sediment at land-water interface (LWI) of the Ganga River in 2020

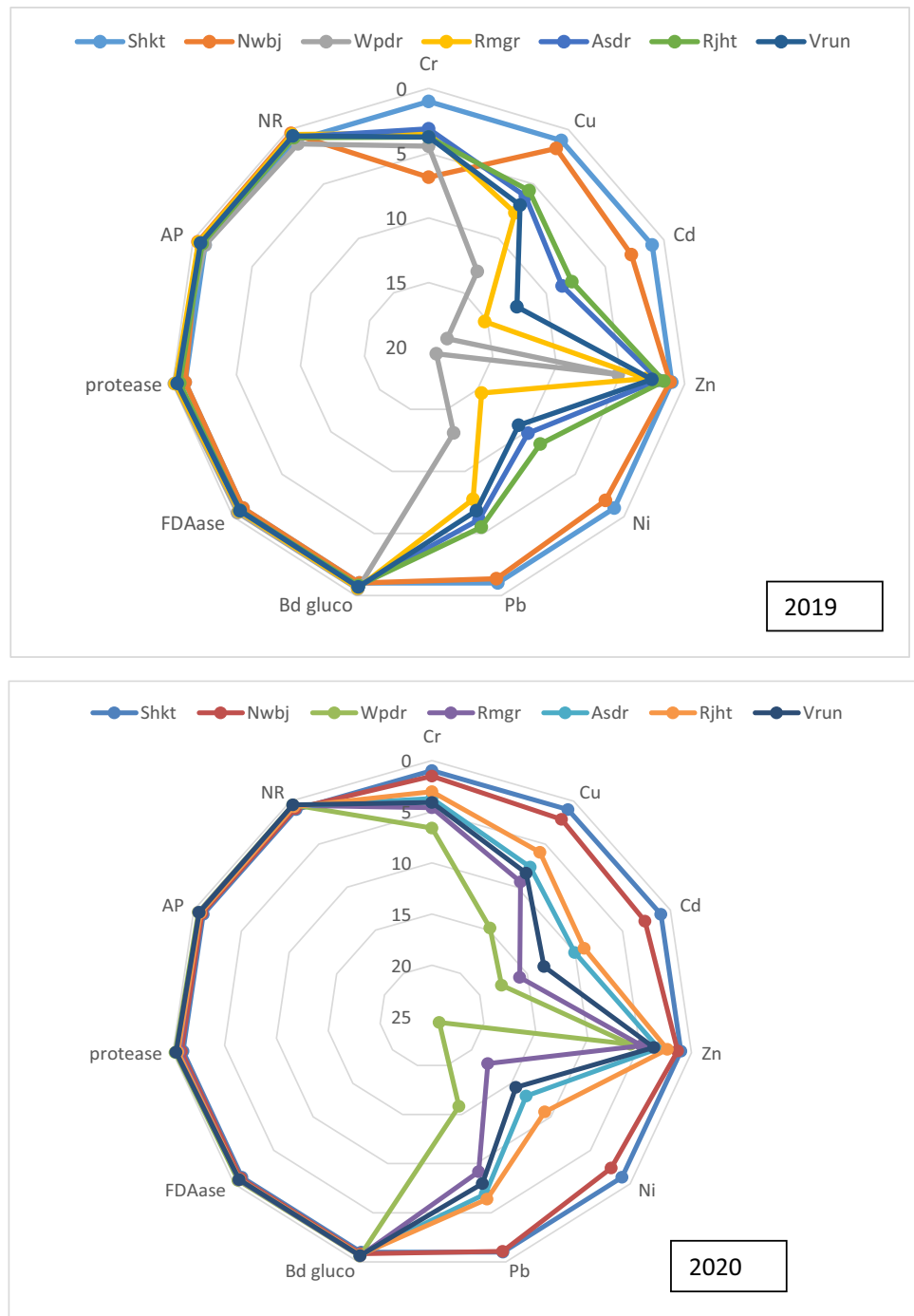
Variable	Slope of covariates				
	b_{TOC}	b_{IN}	B_{DRP}	$b_{\Sigma THM}$	Intercept
B-D-Glu	4.76***	3.28***	0.34**	-0.03***	17.26***
FDAase	2.01***	1.71**	2.02***	-0.02***	10.03**
Protease	0.89***	3.13***	0.78**	-0.02***	10.21**
AP	3.46**	3.42**	-3.87***	-0.04***	11.10***
NR	4.72***	6.59***	5.02***	-0.04***	25.76***

β -D-Glu, β -D-glucosidase; AP, alkaline phosphatase; NR, nitrate reductase; TOC, total organic carbon; IN, inorganic nitrogen ($NO_3^- + NH_4^+$); DRP, dissolved reactive phosphorus (PO_4^{3-}); ΣTHM , total heavy metal. The variance explained by both random (sites) and fixed effects (variables). Codes of significance: $p(>|t|)$: 0 “***”; 0.001 “**”.

during lockdown period. In the Bagmati River (Nepal), the DO level during lockdown period increased by about 1.5 folds (Pant et al. 2021). An improvement in DO_w along

the study stem could be expected due to lack of industrial effluent discharge and closure of commercial activities and small-scale enterprises. These improvements were found

Fig. 8 A multiparametric description using a decagon line (relative to the corresponding value of relatively less polluted site, which thus becomes equal to unity) of selected expressions of some enzyme activities and concentrations of heavy metal in sediment at land-water interface at study sites of the Ganga River



to be more evident at or near industrial discharge locations indicating that industrial flushing sizably contributes to water quality degradation in large rivers and coastal areas (Jaiswal and Pandey 2021a; Selvam et al. 2020). Thus, the closure of industrial activity during lockdown seems to be an important factor responsible for the increasing concentration of DO_w in the Ganga River. Such improvements have been suggested to be used to explore underpinning strategies for the rejuvenation of large rivers (Dutta et al.

2020) and revival of coastal areas (Selvam et al. 2020). The improvements in water quality were witnessed also in terms of decreases in biological oxygen demand (BOD_w). Chakraborty et al. (2021b) reported about 28% decrease in BOD during lockdown period in the Damodar River. Pant et al. (2021) observed about 1.5 and 1.9 time decrease in BOD and COD respectively during lockdown in Bagmati River (Nepal). Similar observations have been made for the Rivers Yamuna (Arif et al. 2021), Tawi (Kour et al. 2021),

Table 4 Dissolved oxygen at sediment-water interface (DO_{sw}) and P release from bottom sediment at different study sites. Values are mean ($n=3$) \pm SE

Site	DO_{sw} (mg L ⁻¹)		Sediment P-release (mg m ⁻² day ⁻¹)	
	2019	2020	2019	2020
	Nwbj	4.30 \pm 0.48	6.75 \pm 0.39	3.00 \pm 0.28
Wpdr	0.37 \pm 0.04	2.15 \pm 0.16	9.90 \pm 0.69	7.27 \pm 0.38
Shtk	6.26 \pm 0.70	7.57 \pm 0.63	1.10 \pm 0.19	0.66 \pm 0.10
Rmgr	3.31 \pm 0.36	4.51 \pm 0.23	5.80 \pm 0.37	4.09 \pm 0.31
Asdr	1.06 \pm 0.18	3.78 \pm 0.23	4.50 \pm 0.43	3.39 \pm 0.25
Rjht	3.00 \pm 0.33	4.04 \pm 0.24	3.50 \pm 0.39	2.85 \pm 0.25
Vrun	1.60 \pm 0.13	2.98 \pm 0.18	7.33 \pm 0.58	5.94 \pm 0.33

and Bhutan-India-Bangladesh trans-boundary rivers (Sarkar et al. 2021). In this study, the effects were relatively less marked at sewage discharge sites although there was a sharp decline in COD particularly at point sources/industrial discharge sites. These changes could be more appropriately witnessed during lockdown period. These observations provide evidence that along with the carbon driven oxygen demand, the other oxygen demanding substances (ODS) are equally responsible for creating the patches of dissolved oxygen deficient zones in many parts of the Ganga River (Jaiswal and Pandey 2019b).

The results showed a clear longitudinal pattern in the concentrations of nutrients (N and P), TOC, and heavy metal pollutants in the river concordant with anthropogenic sources of input entwined with the lockdown effects. The carbon and nutrients did appear the major determinants where urban sewage was the main input source whereas the metal regulators became more important at locations characterized by industrial releases. The concentrations of nutrients, especially those of orthophosphate recorded here, were in the range reported for Yuqiao reservoir of China (Wen et al. 2019). A sharp decline in the concentrations of nutrients and heavy metals in the year 2020 is an indicative of lockdown effect. The improvements were substantial at or near the sites receiving industrial flushing suggesting further a major role of industries in the Ganga River pollution. At the most polluted industrial site (Wpdr), the concentrations of NO_3^- , NH_4^+ , PO_4^- , and TOC declined by 18%, 14%, 17%, and 19% respectively in the 2020 compared to the 2019. For the Damodar River, the concentrations of total phosphorus and nitrate declined by about 70% and 57% respectively during lockdown compared to no-lockdown period (Chakraborty et al. 2021b). In a human-impacted coastal area of Malaysia, Kamarudin et al. (2021) reported about 11.5% decline in nitrate and about 77.2% decline in phosphate under the influence of COVID-19 lockdown. A declining trend was

also observed with respect to the concentration of heavy metals. The Σ THM at the most polluted Wpdr Site declined by 27% in the 2020 compared to the 2019. Similar trend was noticed at other study sites, although at sewage discharge sites, these effects were less pronounced. Kanpur area is an industrial hub and Wazidpur drain receives large input of these effluents from multiple sources. The river at Jajmau and nearby areas receives ~171 mld (million liter per day) municipal sewage (treated:untreated ratio almost 50:50), over 200 mld industrial effluents and about 400 tonnes chemically rich wastes from more than 450 tanneries (CPCB 2013). The treatment systems are not enough to cope-up toxicant removal; thus, the water quality improved in these stretches due to complete shut-down of industrial and commercial activities during lockdown. Chakraborty et al. (2021a) reported upto 50% decline in the concentrations of heavy metals in the Hoogly River Estuary during lockdown period. Karunanidhi et al. (2021) observed about 20 to 38% decline in the concentrations of different heavy metals during lockdown in Thirumanimuthar River. Similar effects of lockdown on heavy metal load and other attributes have been reported by Tokatl and Varol (2021) for Meriç-Ergene River Basin, Turkey. Khan et al. (2021) reported 9.62 to 16.37% reduction in the concentrations of heavy metals in Gomti River during lockdown period. Haghazar et al. (2022) observed about 40% reduction in Cu and 57% reduction in Cr in Zarjoub River (Iran) constrained by COVID-19 lockdown. Our results, as also supported by the other studies, clearly indicate the need of the waste diversion/treatment facilities to minimize the Ganga River pollution.

Dissolved oxygen deficit and sediment-P release

The dissolved oxygen deficit in water (DOD_w) showed a strong synchrony with TOC, a measure of autotrophic-C coupled allochthonous-C flushing. It seemed that the increases in TOC generated strong pressure on dissolved oxygen in water (DO_w), and consequently the DOD_w increased. Accordingly, the variations in DOD_w showed a trend opposite to that of DO_w . During lockdown period, as compared to 2019 values, the DOD_w declined by 25% at Wpdr, 19% at Asdr, and 16% at Vrun. The decreases in DOD_w although varied were recorded irrespective of site. Similar to DOD_w , BOD_w and COD_w declined in the year 2020 at all the study sites, and more sharply at locations characterized by industrial flushing. The mean concentration of DO at sediment-water interface (DO_{sw}) was found above 2.0 mgL⁻¹ in 2020 at all locations, whereas it was well below 2.0 mg L⁻¹ (hereafter called hypoxia) in the year 2019 at Wpdr, Asdr, and Vrun sites. These sites receive concentrated inputs from point sources (Wpdr and Asdr) and a highly polluted urban tributary (Vrun). Our earlier field trials have shown mosaic of hypoxic zones (DO_{sw} below

2.0 mg L⁻¹) at a number of source-oriented sites (Pandey et al. 2019). Lack of benthic hypoxia in 2020, even at locations associated with the point sources and study tributary, suggests a large drop in TOC and other oxygen demanding substances. About 760 grossly polluting industrial units pollute the middle segment of the Ganga River (CPCB 2016). Thus, a sharp improvement in water quality contexting DO_w, DO_{sw}, DOD_w, BOD_w, COD_w, and TOC reflects the effect of COVID-19 lockdown of industrial sector. The stability coefficient (Kardol et al. 2018) was used to ascertain the extent of variations resulting from the factors associated with spatio-temporal determinants by which the differences were administered. The study showed significant decreases ($p < 0.05$) in variances (increased stability coefficient) in the 2020 measurements compared to those recorded in the 2019 suggesting that a decline in variances can be an important attribute to decisively judge a decline in the anthropogenic perturbations. All these evidences indicate that industrial units sizably contribute to the Ganga River pollution.

Because the benthic hypoxia induces ecosystem feedbacks (for instance, Conley et al. 2009), we assessed benthic-sediment P-release as a consequential “response determinant” and a positive feedback to uncover the causal linkages further. The oxygen deficiency at sediment-water interface breaks the Fe-P bond releasing phosphorus from the bed sediment (Middelburg and Levin 2009). In a case study of the Luahe River, China, Zhou et al. (2021) observed a shift from adsorption to desorption at mean soluble reactive phosphorus (SRP) level of 50 µg L⁻¹ suggesting that at 50 µg L⁻¹ or below this concentration of SRP, the river sediment releases P. The hypoxic levels of DO at the sediment-water interface (DO_{sw} < 2.0 mg L⁻¹) were recorded in 2019 at sites such as Wpdr (0.37 mg L⁻¹), Asdr (1.06 mg L⁻¹), and at Vrun (1.60 mg L⁻¹). The magnitude of sediment-P release showed strong asynchrony with the concentration of DO_{sw} indicating concurrence of sediment-P release with oxygen deficiency at sediment-water interface of the river.

The study sites characterized by DO_{sw} < 2.0 mg L⁻¹ did show higher rates of sediment-P release compared to those having oxic or sub-oxic levels of DO_{sw}. Kim et al. (2003) have reported P release at a rate of 100 mg/m²/week from the anaerobic sediments of Han River. However, the sediment-P release recorded in an embayment in Hong Kong was substantially high (Hu et al. 2001). Similar concurrence between DO and sediment-P release has been reported for Hampshire Avon and Herefordshire Wye Rivers, UK (Jarvie et al. 2005); Nansi Lake and its inflow rivers, China (Zhang et al. 2012); Abshineh River, Iran (Jalali and Peikam 2013); and the Ganga River, India (Jaiswal and Pandey 2021a). During the year 2020, none of the study sites showed DO_{sw} < 2.0 mg L⁻¹ and accordingly the sediment-P release remained low. This has relevance and can be treated as a signature of improvement in the system. Because positive feedbacks are

self-enhancing and promote degradation in the river (Jaiswal and Pandey 2021a), our results provide coherent evidence that a declining trend in the sediment-P release, even at most polluted sites, is an indicative of a shift towards recovery. The study shows that the improvement in the level of DO at sediment-water interface and its asynchrony with the ecosystem feedback, such as the sediment-P release as observed during lockdown period, can be used as a “recovery window” to design future strategies for the management and rejuvenation of the large rivers.

Extracellular enzyme activity in sediment

The EE activity in the sediment is considered here as the “response determinants” in two different perspectives. The EE activity was expected to change in response to COVID-19 lockdown-driven reductions in substrates (for instance, carbon and nutrients vs reduction in sewage flushing) and concentrations of heavy metals (vs industrial shutdown). Strong mechanistic links with these response determinants (EE) observed here can help explore river ecosystem functional shifts and recovery windows useful in the management decisions. In this heterogeneously source-flushed river, the industrial releases are the main contributor of metal pollutants. Thus, a significant decline in the metal pollutants provides clear evidence of industrial contribution. Because the river discharge strongly influences the sediment microbial functioning, our study conducted during low flow, characterized almost by a stable hydrological regime coinciding with the lockdown period, shows that the sediment microbial activity followed a great variability in response to changes in the level of carbon, nutrients, and heavy metals along the river continuum. To validate these issues, we used EE activities as an ecotoxicological response determinant and as an indicator of industrial shutdown-associated changes in metal pollution load. Both NMDS and multiparametric descriptive statistics segregated EE activities opposite to metal pollutants. The EE activities help extrapolating community level physiological profile, bacterial community composition, and carbon substrate in the river continuum (Freixa et al. 2016). These proximate agents of decomposition of organic matter can be used to re-construct the microbial assimilation pathways as well as the rates of microbial metabolism (Sinsabaugh et al. 2009, 2016). Here, entwined with improvement in DO_{sw} in 2020, the result showed a significant increase in alkaline phosphatase (AP) activity. An improvement in response attributes such as AP activity is an indicator of recovery windows, for instance, indicative of reduced metal toxicity (Jaiswal and Pandey 2018), reduced P-flushing (Pandey and Yadav 2017), and reduced sediment-P release (Jaiswal and Pandey 2021a). Phosphate is a pH independent competitive inhibitor of AP enzyme (Coleman 1992), and an improvement in AP activity is an

indicative of reduced phosphate loading from external as well as internal (sediment P-release) sources. Also, alkaline phosphatase is highly sensitive to heavy metals, especially towards Cd and Cu that replace the native Zn from the active site and/or disturb its 3D structure (Coleman 1992; Poirier et al. 2008). Our earlier studies show that, at C poor locations, total heavy metal (ΣTHM) concentration in the sediment exceeding $347.44 \mu\text{g g}^{-1}$ caused significant inhibitory effect on EE activity. At C-rich sites, inhibitory effects have been seen at $\Sigma\text{THM} > 472.53 \mu\text{g g}^{-1}$ (Jaiswal and Pandey 2019a). In this study, ΣTHM exceeded $610 \mu\text{g g}^{-1}$ and $368 \mu\text{g g}^{-1}$ at Wpdr and Vrun sites respectively in the year 2019 which reduced significantly in the 2020. Jaiswal and Pandey (2019b) did observe strong negative correlation of AP with soluble reactive phosphate and heavy metals measured in a long stretch of the Ganga River. Other EEs — β -D-glucosidase, protease, and FDAase — showed a marked decline in response to spatio-temporal variations in the concentrations of heavy metals in the 2019 with an improvement in the 2020. Also, because β -D-glucosidase is a proximate agent of C-acquisition (Sinsabaugh et al. 2009), an increase in β -D-glucosidase activities in the middle reaches reflects the effect of inputs from anthropogenic tributaries/urban flushing that increase the quantity of easily degradable organic carbon. The FDAase is used as a proximate agent of total microbial activity (Costa et al. 2007). This hydrolytic process involves all the three groups of enzymes — esterase, lipase, and protease and hence used as a measure of a holistic assay (Schnürer and Rosswall 1982). An increase in FDAase activity in the year 2020, especially at sites releasing metal pollutants, indicates a lockdown-associated reduction in heavy metal toxicity. During non-lockdown period, Jaiswal and Pandey (2019c) observed significant negative correlation between FDAase and ΣTHM at C poor metal-polluted sites, where FDAase activity ranged from 34.09 to $115.98 \mu\text{g fluorescein g}^{-1} \text{h}^{-1}$. Protease hydrolyses the peptide bonds of proteins into peptides and amino acids. Heavy metals may elicit negative effects on protease activity by interfering with sulfhydryl group at catalytic site or by forming complexes with the amino acids (Muñoz et al. 2012; Huang et al. 2015).

As expected, the metabolic measure of stress condition — microbial metabolic quotient — increased almost synchronously to the metal concentrations. High activities of enzymes, except AP at Asdr, reflect the influence of nutrient and carbon-rich sewage flushing. At this site, a point source drains a large amount (66.4 MLD) of municipal sewage, rich in easily degradable organic matter, directly to the river. Also, nutrient enrichment favors the development of biofilm, and consequently, provides labile carbon for microbial heterotrophs (Battin et al. 2016). On the contrary, the discharge inputs from Wazidpur drain are rich in heavy metals and consequently inhibit EE activities. These results suggest

that the proportion of OM and the concentration of heavy metals can be directly linked with changes in EE activities in the river continuum. However, the collateral effects, such as those expected at site locations characterized by parallel entry of carbon, nutrients, and heavy metals, can change the overall effects to constrain the prediction of a specific response. For instance, C enrichment enhances EE activity, whereas accumulation of metal stressors tends to counterbalance these effects. A comparison of 2020 results (lockdown period) with their 2019 counterparts presented here supports these assertions. High concentration of heavy metals in 2019 outweighed the positive effects of nutrients and carbon enrichment on EE activities. This disconnected pattern or weak coupling between OM and EE activities has also been reported in our previous studies (Jaiswal and Pandey 2018, 2019 a,b). In the present study, the counterbalancing effects were reduced concurrent with reduction in metal pollutants during lockdown period.

To move a step ahead, we computed stability coefficients for the total metal pollutants and EE variables. The results showed synchronous spatio-temporal oscillations with stability coefficient being lower at source oriented/disturbed locations. Because the metal and carbon releases vary subject to the nature of the source input, the spatial trends in stability coefficient further support our contention. The study further considered the generalized linear mixed model (GLMM) to compare the results. The GLMM analyses showed significant relationships between the variables, being strongly negative with heavy metals. Also, the AP activity correlated negatively with dissolved reactive P. In general, the relationships were stronger in the year 2019. To support our assertion further, correlative evidences were collected to link these functional attributes with causal determinants. Relatively weaker correlations ($R^2 < 0.75$) between the concentration of the total heavy metals (ΣTHM) and EE activities during lockdown period indicated relatively weak effect of metal pollutants and have relevance in a sediment-based ecotoxicological perspective.

Conclusions

The study showed that COVID-19 shutdown of the industrial and other activities caused considerable improvement in water and sediment quality of the Ganga River. The concentration of dissolved oxygen in water (DO_w) varied between 1.8 and 7.4 mg L^{-1} in the year 2019 which improved in the year 2020 with values ranging from 2.2 to 8.5 mg L^{-1} . Even the source-oriented locations did not show a single value close to benthic hypoxia (DO_w below 2.0 mg L^{-1}) in the year 2020 as observed at Wpdr during the 2019 (non-lockdown period). At Wpdr (an industrial point source site), TOC, NO_3^- , NH_4^+ , and PO_4^{3-} in the

sediment declined by 21.28, 34.34, 17.84, and 22.06% respectively in the 2020 compared to the year 2019. The concentration of total heavy metal (Σ THM) in the sediment exceeded $610 \mu\text{g g}^{-1}$ and $368 \mu\text{g g}^{-1}$ at Wpdr and Vrun sites respectively in the year 2019 which reduced significantly in the 2020 (the lockdown period). The Σ THM at Wpdr declined by 34.28% in the 2020 compared to the 2019. Response determinants — sediment-P release, CO_2 emission, and EE activities — also showed improvement during “clean” days witnessing reduced concentration of the heavy metals. It is important to note that despite a decline in carbon, a substrate for EE activity, lowered concentrations of heavy metals opened a recovery window for the EE activities to increase. The study has relevance in three different context: First, the present evaluation is important because an accurate assessment of the influence of source-release-control measures and causal connections thereof is unlikely in near future due to lack of a “control” similar to those occurred during COVID-19. Second, based on water and sediment quality changes and correlative evidences with response determinants, the study shows that the industrial releases are important contributor of metal pollution in the Ganga River. Third, the study opens a way to uncover the recovery windows (reduced sediment-P release and reduced metal toxicity in terms of EE activity etc.) for management decisions so that a river ecosystem can be channeled to recover and rebound from perturbations.

Acknowledgements The authors are thankful to Head, Department of Botany, Banaras Hindu University, for facilities. We also thank Mr. Vikash Barnwal, Department of Statistics Institute of Science, BHU, Varanasi, for assistance in statistical analysis.

Author contribution Madhulika Singh: sample collection and formal analysis, methodology, data validation, writing original draft, visualization, and funding acquisition. Usha Pandey: hypothesis, experimental design, review and editing, visualization. Jitendra Pandey: conceptualization and hypothesis, observation, writing, review and editing, validation, visualization, project management, and supervision.

Funding This study was fully funded by University Grant Commission (Grant No. DSKPDF-BL/18-19/0173) for funding support to Dr. Madhulika Singh as a Dr. D. S. Kothari Post-Doctoral Fellow.

Data availability All data generated or analyzed during this study are included in this published article.

Declarations

Ethical approval Not applicable.

Consent to participate Not applicable.

Consent for publication Not applicable.

Competing interests The authors declare no competing interests.

References

- Adam G, Duncan H (2001) Development of a sensitive and rapid method for the measurement of total microbial activity using fluorescein diacetate (FDA) in a range of soils. *Soil Biol Biochem* 33:943–951
- Allen SE, Grimshaw HM, Rowland AP (1986) Chemical analysis. In: Moore PD, Chapman SB (eds) *Methods in plant ecology*. Blackwell Scientific Publication, Oxford, London, pp 285–344
- Anderson JPE, Domsch KH (1978) A physiologically active method for the quantitative measurement of microbial biomass in soils. *Soil Biol Biochem* 10:215–221
- APHA (1998) *Standard methods for the examination of water and wastewater*. American Public Health Association, Washington, DC
- Arif M, Kumar R, Parveen S (2021) Reduction in water pollution in Yamuna River due to lockdown under COVID-19 pandemic.
- Battin TJ, Besemer K, Bengtsson MM, Romani AM, Packmann AI (2016) The ecology and biogeochemistry of stream biofilms. *Nat Rev Microbiol* 14:251–263
- Bournaud M, Cellot B, Richoux P, Berrahou A (1996) Macroinvertebrate community structure and environmental characteristics along a large river: congruity of patterns for identification to species or family. *J North Am Benthol Soc* 15:232–253
- Breslow NE, Clayton DG (1993) Approximate inference in generalized linear mixed models. *J Am Statist Assoc* 88:9–25
- Brookes PC, Powlson DS, Jenkinson DS (1982) Measurement of microbial biomass phosphorus in soil. *Soil Biol Biochem* 14:319–329
- Carpenter SR, Brock WA (2006) Rising variance: a leading indicator of ecological transition. *Ecol Lett* 9:311–318
- Central Pollution Control Board (2013) *Pollution assessment: River Ganga*. Ministry of Environment and Forests, Govt. of India, Parivesh Bhawan, Delhi
- Central Pollution Control Board (2016) *Bulletin Vol-I*. Ministry of Environment and Forests, Govt. of India, Parivesh Bhawan, Delhi
- Chakraborty B, Bera B, Adhikary PP, Bhattacharjee S, Roy S, Saha S, Ghosh A, Sengupta D, Shit PK (2021b) Positive effects of COVID-19 lockdown on river water quality: evidence from River Damodar, India. *Scientific Rep* 11:1–16
- Chakraborty S, Sarkar K, Chakraborty S, Ojha A, Banik A, Chatterjee A, Ghosh S, Das M (2021a) Assessment of the surface water quality improvement during pandemic lockdown in ecologically stressed Hooghly River (Ganges) Estuary, West Bengal, India. *Mar Pollut Bull* 171:112711
- Chapman D (1996) *Water quality assessment: a guide to the use of biota, sediments and water in environmental monitoring*, 2nd edn. E and FN Spon, London
- Ciavatta C, Govil M, Antisari VL, Sequi P (1991) Determination of organic carbon in aqueous extract of soil and fertilizers. *Commun Soil Sci Plant Anal* 22:795–807
- Coleman JE (1992) Structure and mechanism of alkaline phosphatase. *Annu Rev Biophys Biomol Struct* 21:441–483
- Conley DJ, Carstensen J, Vaquer-Sunyer R, Duarte CM (2009) Ecosystem thresholds with hypoxia. In *Eutrophication in coastal ecosystems*. Springer, Dordrecht, pp 21–29
- Costa AL, Paixão SM, Caçador I, Carolin M (2007) CLPP and EEA profiles of microbial communities in salt marsh sediments. *J Soils Sediments* 7:418–425
- Doherty M, Yager PL, Moran MA, Coles VJ, Fortunato CS, Krusche AV, Medeiros PM, Payet JP, Richey JE, Satinsky BM, Sawakuchi HO, Ward ND, Crump BC (2017) Bacterial biogeography across the Amazon River-ocean continuum. *Front Microbiol* 8:882
- Dutta V, Dubey D, Kumar S (2020) Cleaning the River Ganga: impact of lockdown on water quality and future implications on river rejuvenation strategies. *Sci Total Environ* 743:140756

- Eaton AD, Clesceri LS, Greenberg AE (1995) Standard methods for the examination of water and wastewater, 19th edn. American Public Health Association, USA
- Eivazi F, Tabatabai MA (1988) Glucosidase and galactosidases in soils. *Soil Biol Biochem* 20:601–606
- Fazi S, Vázquez E, Casamayor EO, Amalfitano S, Butturini A (2013) Stream hydrological fragmentation drives bacterioplankton community composition. *PLoS one* 8:e64109
- Freixa A, Ejarque E, Crognale S, Amalfitano S, Fazi S, Butturini A, Romani AM (2016) Sediment microbial communities rely on different dissolved organic matter sources along a Mediterranean river continuum. *Limnol Oceanography* 61:1389–1405
- Gard V, Aggrawal SP, Chauhan P (2020) Changes in turbidity along Ganga River using sentinel-2 satellite data during lockdown associated with COVID-19. *Geomat Nat HazRisk* 11:1175–1195
- Global Carbon Project: Carbon Brief (2020) <https://www.globalcarbonproject.org/carbonbudget/archive.htm>
- Häder DP, Banaszak AT, Villafañe VE, Narvarte MA, González RA, Helbling EW (2020) Anthropogenic pollution of aquatic ecosystems: emerging problems with global implications. *Sci Total Environ* 713:136586
- Haghnazar H, Cunningham JA, Kumar V, Aghayani E, Mehraein M (2022) COVID-19 and urban rivers: effects of lockdown period on surface water pollution and quality—a case study of the Zarjoub River, north of Iran. *Environ Sci Pollut Res*:1–17
- Hill BH, Elonen CM, Jicha TM, Bolgrien DW, Moffett MF (2010) Sediment microbial enzyme activity as an indicator of nutrient limitation in the great rivers of the Upper Mississippi River basin. *Biogeochemistry* 97:195–209
- Hu WF, Lo W, Chua H, Sin SN, Yu PHF (2001) Nutrient release and sediment oxygen demand in a eutrophic land-locked embayment in Hong Kong. *Environ Int* 26:369–375
- Huang D, Xu J, Zeng G, Lai C, Yuan X, Luo X, Xu P, Huang C (2015) Influence of exogenous lead pollution on enzyme activities and organic matter degradation in the surface of river sediment. *Environ Sci Pollut Res* 22:11422–11435
- Jaiswal D, Pandey J (2018) Impact of heavy metal on activity of some microbial enzymes in the riverbed sediments: ecotoxicological implications in the Ganga River (India). *Ecotoxicol Environ Saf* 150:104–115
- Jaiswal D, Pandey J (2019b) Anthropogenically enhanced sediment-oxygen demand creates mosaic of oxygen deficient zones in the Ganga River: implications for river health. *Ecotoxicol Environ Saf* 171:709–720
- Jaiswal D, Pandey J (2019c) An ecological response index for simultaneous prediction of eutrophication and metal pollution in large rivers. *Wat Res* 161:423–438
- Jaiswal D, Pandey J (2021a) Human-driven changes in sediment-water interactions may increase the degradation of ecosystem functioning in the Ganga River. *J Hydrol* 598:126261
- Jaiswal D, Pandey J (2019a) Carbon dioxide emission coupled extracellular enzyme activity at land-water interface predict C-eutrophication and heavy metal contamination in Ganga River, India. *Ecol Indic* 99:349–364
- Jaiswal D, Pandey J (2021b) River ecosystem resilience risk index: a tool to quantitatively characterize resilience and critical transitions in human-impacted large rivers. *Environ Pollut* 268:115771
- Jaiswal D, Pandey U, Mishra V, Pandey J (2021) Integrating resilience with functional ecosystem measures: a novel paradigm for management decisions under multiple-stressor interplay in freshwater ecosystems. *Glob Change Biol* 27:3699–3717
- Jalali M, Peikam EN (2013) Phosphorus sorption-desorption behaviour of river bed sediments in the Abshineh river, Hamedan, Iran, related to their composition. *Environ Monit Assess* 185:537–552
- Jarvie HP, Jürgens MD, Williams RJ, Neal C, Davies JJ, Barrett C, White J (2005) Role of river bed sediments as sources and sinks of phosphorus across two major eutrophic UK river basins: the Hampshire Avon and Herefordshire Wye. *J Hydrol Nutrient Mobil River Basins: A Eur Perspective* 304:51–74
- Jenkinson D, Powlson DS (1976) The effects of biocidal treatments on metabolism in soil – V: a method for measuring soil biomass. *Soil Biol Biochem* 8:209–213
- Kamarudin NA, Mohamat-Yusuff F, Zulkifli SZ, Zainuddin AH, Ali MY, Ekhsan NFM, Hassan MZ, Aris AZ, Yusoff FM (2021) Port Dickson surface water quality status: a year with COVID-19 pandemic. In *IOP Conference Series: Earth Environ Sci* 934:012049
- Kardol P, Famin N, Wardle DA (2018) Long-term effects of species loss on community properties across contrasting ecosystems. *Nature* 557:710–713
- Karunanidhi D, Aravinthasamy P, Subramani T, Setia R (2021) Effects of COVID-19 pandemic lockdown on microbial and metals contaminations in a part of Thirumanimuthar River, South India: a comparative health hazard perspective. *J Hazard Mater* 416:125909
- Khan R, Saxena A, Shukla S, Sekar S, Goel P (2021) Effect of COVID-19 lockdown on the water quality index of River Gomti, India, with potential hazard of faecal-oral transmission. *Environ Sci Pollut Res*:1–9
- Kim LH, Choi E, Stenstrom MK (2003) Sediment characteristics, phosphorus types and phosphorus release rates between river and lake sediments. *Chemosphere* 50:53–61
- Kobayashi Y, Kim C, Yoshimizu C, Kohzu A, Tayasu I, Nagata T (2009) Longitudinal changes in bacterial community composition in river epilithic biofilms: influence of nutrients and organic matter. *Aquatic Microbial Ecol* 54:135–152
- Kour G, Kothari R, Dhar S, Pathania D, Tyagi VV (2021) Impact assessment on water quality in the polluted stretch using a cluster analysis during pre-and COVID-19 lockdown of Tawi river basin, Jammu, North India: an environment resiliency. *Energy Ecol Environ*:1–12
- Ladd JN, Buttler HA (1972) Short-term assays of soil proteolytic enzyme activities using proteins and dipeptide derivatives as substrates. *Soil Biol Biochem* 4:19–30
- Luo L, Meng H, Gu JD (2017) Microbial extracellular enzymes in biogeochemical cycling of ecosystems. *J Environ Manag* 197:539–549
- Manzoni S, Jackson RB, Trofymow JA, Porporato A (2008) The global stoichiometry of litter nitrogen mineralization. *Science* 321:684–686
- Maranger RJ, Pace ML, Del Giorgio PA, Caraco N, Cole JJ (2005) Longitudinal spatial patterns of bacterial production and respiration in a large river-estuary: implications for ecosystem carbon consumption. *Ecosystems* 8:318–330
- Michel P (1984) Ecological methods for field and laboratory investigation. Tata McGraw-Hill Publication Company, New Delhi
- Middelburg JJ, Levin LA (2009) Coastal hypoxia and sediment biogeochemistry. *Biogeosciences* 6:1273–1293
- Muñoz AJ, Ruiz E, Abriouel H, Gálvez A, Ezzouhri L, Lairini K, Espínola F (2012) Heavy metal tolerance of microorganisms isolated from wastewaters: identification and evaluation of its potential for biosorption. *Chem Eng J* 210:325–332
- Murphy J, Riley J (1962) A modified single solution method for the determination of phosphate in natural waters. *Anal Chim Acta* 27:31–36
- Nowak J, Kaklewski K, Klodka D (2002) Influence of various concentrations of selenic acid (IV) on the activity of soil enzymes. *Sci Total Environ* 291:105–110
- Pandey J, Jaiswal D, Pandey U (2019) Point source-driven seasonal hypoxia signals habitat fragmentation and ecosystem change in River Ganga. *Curr Sci* 117:1947–1949

- Pandey J, Yadav A (2017) Alternative alert system for Ganga river eutrophication using alkaline phosphatase as a level determinant. *Ecol Indic* 82:327–343
- Pant RR, Bishwakarma K, Qaiser FUR, Pathak L, Jayaswal G, Sapkota B, Pal KL, Thapu LB, Koirala M, Rijal K, Maskey R (2021) Imprints of COVID-19 lockdown on the surface water quality of Bagmati river basin. Nepal. *J Environ Manage* 289:112522
- Park G, Oh H, Ahn S (2009) Improvement of the ammonia analysis by the phenate method in water and wastewater. *Bull Korean Chem Soc* 30:2032–2038
- Poirier I, Jean N, Guary JC, Bertrand M (2008) Responses of the marine bacterium *Pseudomonas fluorescens* to an excess of heavy metals: physiological and biochemical aspects. *Sci Total Environ* 406:76–87
- Sánchez E, Colmenarejo MF, Vicente J, Rubio A, García MG, Travieso L, Borja R (2007) Use of the water quality index and dissolved oxygen deficit as simple indicators of watersheds pollution. *Ecol Indic* 7:315–328
- Sarkar S, Roy A, Bhattacharjee S, Shit PK, Bera B (2021) Effects of COVID-19 lockdown and unlock on health of Bhutan-India-Bangladesh trans-boundary rivers. *J Hazard Mater Adv* 4:100030
- Savio D, Sinclair L, Ijaz UZ, Parajka J, Reischer GH, Stadler P, Blaschke AP, Blöschl G, Mach RL, Kirschner AKT, Farnleitner AH, Eiler A (2015) Bacterial diversity along a 2600 km river continuum. *Environ Microbiol* 17:4994–5007
- Schimel JP, Weintraub MN (2003) The implications of exoenzyme activity on microbial carbon and nitrogen limitation in soil: a theoretical model. *Soil Biol Biochem* 35:549–563
- Schnürer J, Rosswall T (1982) Fluorescein diacetate hydrolysis as a measure of total microbial activity in soil and litter. *Applied and environmental microbiology* 43:1256–1261
- Selvam S, Jesuraja K, Venkatramanan S, Chung SY, Roy PD, Muthukumar P, Kumar M (2020) Imprints of pandemic lockdown on subsurface water quality in the coastal industrial city of Tuticorin, South India: a revival perspective. *Sci Total Environ* 738:139848
- Shen SM, Pruden G, Jenkinson DS (1984) Mineralization and immobilization of nitrogen in fumigated soil and the measurement of microbial biomass nitrogen. *Soil Biol Biochem* 16:437–444
- Sinsabaugh RL, Carreiro MM, Repert DA (2002) Allocation of extracellular enzymatic activity in relation to litter composition, N deposition, and mass loss. *Biogeochemistry* 60:1–24
- Sinsabaugh RL, Hill BH, Shah JF (2009) Ecoenzymatic stoichiometry of microbial organic nutrient acquisition in soil and sediment. *Nature* 462:795–798
- Sinsabaugh RL, Turner BL, Talbot JM, Waring BG, Powers JS, Kuske CR, Moorhead DL, Follstad Shah JJ (2016) Stoichiometry of microbial carbon use efficiency in soils. *Ecol Monogr* 86:172–189
- Tabatabai MA, Bremner JM (1969) Use of p-nitrophenyl phosphate for assay of soil phosphatase activity. *Soil Biol Biochem* 1:301–307
- Tokatlı C, Varol M (2021) Impact of the COVID-19 lockdown period on surface water quality in the Meriç-Ergene River Basin. Northwest Turkey. *Environ Res* 197:111051
- Vannote RL, Minshall GW, Cummins KW, Sedell JR, Cushing CE (1980) The river continuum concept. *Can J Fish Aquat Sci* 37:130–137
- Wallace JB, Eggert SL, Meyer JL, Webster JR (1997) Multiple trophic levels of a forest stream linked to terrestrial litter inputs. *Science* 277:102–104
- Wardle DA, Yeates GW, Watson RN, Nicholson KS (1993) Response of soil microbial biomass and plant litter decomposition in maize and asparagus cropping systems. *Soil Biol Biochem* 25:857–868
- Wen SL, Wu T, Yang J, Jiang X, Zhong JC (2019) Spatio-temporal variation in nutrient profiles and exchange fluxes at the sediment-water interface in Yuqiao Reservoir, China. *Int J Environ Res Public Health* 16:3071
- World Health Organization (2020) Mental health and psychosocial considerations during the COVID-19 outbreak, 18 March 2020 (No. WHO/2019-nCoV/MentalHealth/2020.1). World Health Organization
- Yunus AP, Masago Y, Hijioka Y (2020) COVID-19 and surface water quality: improved lake water quality during the lockdown. *Sci Total Environ* 731:139012
- Zeglin LH (2015) Stream microbial diversity in response to environmental changes: review and synthesis of existing research. *Front Microbiol* 6:454
- Zhang ZB, Tan XB, Wei LL, Yu SM, Wu DJ (2012) Comparison between the lower Nansi Lake and its inflow rivers in sedimentary phosphorus fractions and phosphorus adsorption characteristics. *Environ Earth Sci* 66:1569–1576
- Zhou B, Fu X, Wu B, He J, Vogt RD, Yu D, Yue F, Chai M (2021) Phosphorus release from sediments in a raw water reservoir with reduced allochthonous input. *Water* 13:1983
- Zoppini A, Ademollo N, Amalfitano S, Casella P, Patrolecco L, Polesello S (2014) Organic priority substances and microbial processes in river sediments subject to contrasting hydrological conditions. *Sci Total Environ* 484:74–83

Publisher's note Springer Nature remains neutral with regard to jurisdictional claims in published maps and institutional affiliations.